FINITE ELEMENT ANALYSIS OF HISTORIC BRIDGE STRENGTENED WITH FRP LAMINATES

Damian I. Kachlakev, Ph.D., P.E.
California Polytechnic State University

Abstract

A three-dimensional finite element model is developed to examine the structural behavior of the Horsetail Creek Bridge in Oregon both before and after applying FRP laminates. Nonlinear finite element analysis is performed using the ANSYS program. SOLID65, LINK8, and SOLID46 elements represent concrete, discrete reinforcing steel bars, and FRP laminates, respectively. Based on each component's actual characteristics, nonlinear material properties are defined for the first two types of elements. Truck loadings are applied to the FE bridge model at different locations, as in the actual bridge test. The comparisons between ANSYS predictions and field data are made in terms of concrete strains. The analysis shows that the FE bridge model does not crack under the applied service truckloads. The FE bridge model very well predicts the trends in the strains versus the various truckload locations. In addition, effects of FRP strengthening on structural performance of the bridge are observed in the linear range.

KEY WORDS: Nonlinear Finite Element Analysis, Fiber-Reinforced Polymer, Bridges

Introduction

Many of the nation's bridges are in need of strengthening. The need for strengthening arises when there is an increase in load requirements, a change in use, or a corrosion problem. The Horsetail Creek Bridge (HCB) was an example of a bridge classified as structurally deficient ([1], [2]). The bridge was not designed to carry the traffic loads that are common today. The bridge was rated and was found to have only 6% of the required shear capacity for the transverse beams and only 34% for the longitudinal beams due to the absence of shear stirrups in both beams and approximately 50% of the required flexural capacity for the transverse beams [3].

One of the potential solutions to increase the load-carrying capacity of the bridge is to strengthen the structure with fiber-reinforced polymer (FRP) materials. FRP sheets were laminated to the bridge where the structural capacity was insufficient. Both transverse and longitudinal beams of the bridge were strengthened due to the deficiencies in shear and flexural capacities. In the case of the transverse beams, both shear and flexural strengthening were required, while only shear strengthening was needed for the longitudinal beams. That is, CFRP (Carbon-FRP) flexural and GFRP (Glass-FRP) shear laminates were attached at the bottom and at the sides of the transverse beams, respectively, while only GFRP laminates were attached at the sides of the longitudinal beams.

In this paper, three-dimensional finite element bridge models are developed to replicate the HCB before and after FRP strengthening using the finite element method (FEM). Modeling methodology and nonlinear analysis approach in ANSYS are presented. The results obtained from the FE bridge model are compared with the field test data in terms of strains on the transverse beam versus various truckload locations on the bridge deck. In addition, the study of effects of FRP strengthening is made.

FE Modeling Methodology and Nonlinear Analysis Approach in ANSYS

Three materials are involved in the bridge structures in this study; i.e., concrete, steel, and FRP.

Concrete: The SOLID65, 3-D reinforced concrete solid, is used to represent concrete in the models. The element using a $2\times2\times2$ Gaussian set of integration points is defined by eight nodes having three degrees of freedom at each node: translations in the nodal x, y, and z directions. This element is capable of cracking in tension and crushing in compression. Cracking is treated as a "smeared band" of cracks, rather than discrete cracks in ANSYS [4] and occurs as soon as stresses in the concrete exceed the tensile strength of the material. For the modeling of crushing, the material is assumed to crush if all principal stresses are in compression, when the material at an integration point fails in uniaxial, biaxial, or triaxial compression [4]. However, the crushing capability of the SOLID65 element is turned off in this study to avoid a "rapid collapse" in the FE simulation. This element can model concrete with or without reinforcing bars. If the rebar capability is used, the bars will be smeared throughout the element. Nevertheless, in this study a discrete bar element is used instead of the smeared reinforcing approach. The most important aspect of the SOLID65 element is the treatment of nonlinear material properties. The response of concrete under loading is characterized by a distinctly nonlinear behavior. The typical behavior expressed in the stress-strain relationship for concrete subjected to uniaxial loading is shown in Fig. 1.

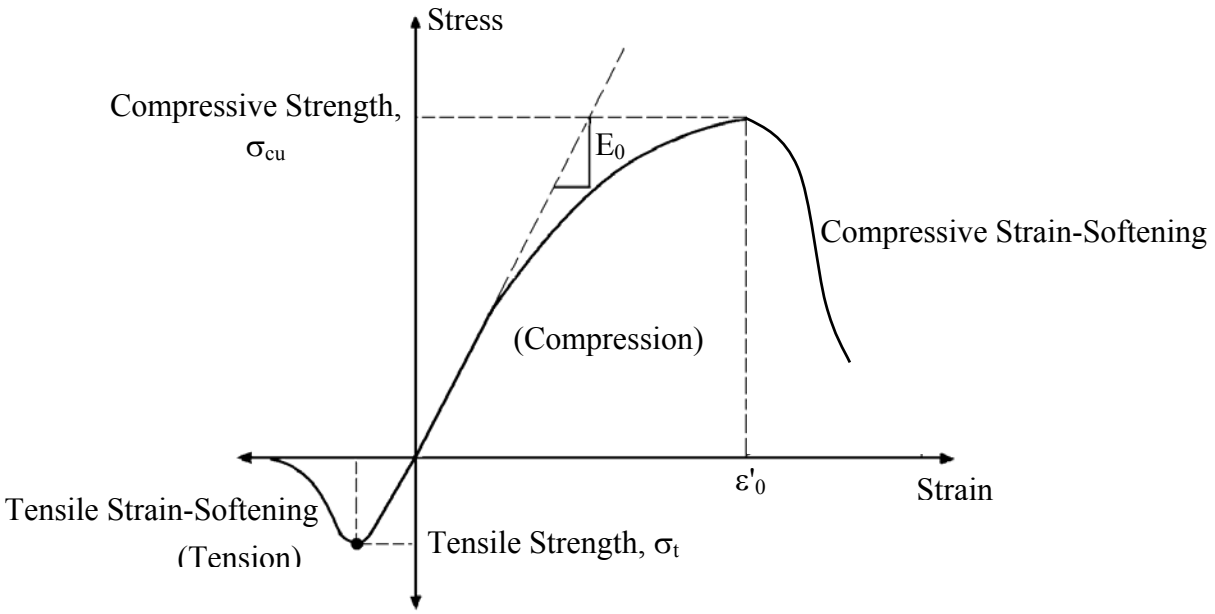

Fig. 1: Typical concrete behavior under uniaxial loading [5].

Uniaxial tensile and compressive strengths (σ_{cu} and σ_t) and uniaxial nonlinear stress-strain relationship for concrete are defined as parts of the material properties in the SOLID65 element. The first two parameters are required to define failure surface for the concrete due to a multiaxial stress state [6]. The uniaxial tensile strength, σ_t, can be calculated, based on [7]:

$$\sigma_t = 0.623\sqrt{\sigma_{cu}} \quad \text{(MPa)} \qquad [1]$$

Many numerical expressions have been developed to express the stress-strain relationships for concrete under different types of loading conditions. However, the constitutive model for concrete under uniaxial compression used in this study is given in [5]. For the ascending portions of the curve in compression, the stress-strain relationship is given as follows:

$$\sigma = \frac{E_0 \varepsilon}{1 + \left(\frac{\varepsilon}{\varepsilon'_0}\right)^2} \qquad [2]$$

$$\varepsilon'_0 = 2\frac{\sigma_{cu}}{E_0} \qquad [3]$$

$$E_0 = 4733\sqrt{\sigma_{cu}} \quad \text{(MPa)} \qquad [4]$$

A perfectly plastic relationship is used instead of the compressive strain-softening curve in this study. Under uniaxial tension, the material is assumed to be linearly elastic with a modulus of elasticity of E_0 up to the tensile strength.

Reinforcing Steel Bars: The LINK8, 3-D spar element, is used to represent the reinforcing steel bar. It is a uniaxial tension-compression that can also include nonlinear material properties. Two nodes having three degrees of freedom at each node, as in the SOLID65 element, define the element. The elastic-perfectly plastic representation is assumed for the reinforcing steel bars in this study.

FRP Laminates: The SOLID46, 3-D layered structural solid element, is used to represent the FRP materials. This element allows up to 250 different material layers. Eight nodes having three degrees of freedom at each node, as in the SOLID65 element, define the element. Layer thickness, layer material direction angles, and orthotropic material properties also need to be defined. No slippage is assumed between the element layers (perfect interlaminate bond). FRP laminates are brittle materials. The stress-strain relationship is roughly linear up to failure. In the nonlinear analysis of the large-scale transverse beams ([8], [9]), no FRP elements show a stress higher than their ultimate strength. Consequently, in this study it is assumed that the stress-strain relationships for the FRP laminates are linearly elastic.

A summary of the material properties used for each component in the FE bridge model is shown in Table 1.

Table 1: Material properties ([10], [11])

Type of Material	Material Properties				
	ν	E MPa	G MPa	Strength MPa	Thickness mm
Concrete	0.2	19650	-	σ_{cu} = 17.24** σ_t = 2.586	-
Reinforcing steel	0.3	199900**	-	fy = 275.8**	-
CFRP laminate	ν_{12} = 0.216 ν_{13} = 0.216 ν_{23} = 0.3*	E_{11} = 62050 E_{22} = 4826* E_{33} = 4826*	G_{12} = 3266* G_{13} = 3266* G_{23} = 1862***	$\sigma_{ult(ten.)}$ = 958.4 $\sigma_{ult(comp.)}$ = 599 $\tau_{ult(12)}$ = 99.97	1.067
GFRP laminate	ν_{12} = 0.216 ν_{13} = 0.216 ν_{23} = 0.3*	E_{11} = 20680 E_{22} = 6895* E_{33} = 6895*	G_{12} = 1517 G_{13} = 1517 G_{23} = 2654***	$\sigma_{ult(ten.)}$ = 599.8 $\sigma_{ult(comp.)}$ = 333.2 $\tau_{ult(12)}$ = 30.34	1.321

Notes: * [12]** [3] for the bridge built prior to 1959. *** $G_{23} = \frac{E_2}{2(1+\upsilon_{23})}$

Modeling Modifications

To make the FE models more efficient when analyzed in ANSYS and to reduce the model complexity, run-time, and memory requirements, modeling modifications were made for the HCB as follows:

Equivalent Thickness of FRP Laminates

The HCB is retrofitted with several different combinations of both CFRP and GFRP laminates in order to resist the expected bending moments and shear forces, respectively. This of course induces non-uniformity in the thickness, which leads to a modeling difficulty. With the special layer modeling capacity in the SOLID46 (FRP) element, a portion of the structure consisting of different materials and fiber orientations is represented using one SOLID46 element. Moreover, the thickness of the FRP laminates, which varies along the actual bridge, can be kept constant using equivalent thickness modeling. For example, when half reduces the original laminate thickness, the modulus of elasticity (E) and shear modulus (G) in all three directions are doubled, and vise versa. Poisson's ratios are independent of the thickness of laminate; therefore, they are kept the same throughout.

"Lumping" of Reinforcing Steel Bar Areas

In addition to the several different combinations of the FRP laminates, the HCB also consists of many steel reinforcement details. To be able to limit the number of elements effectively, at the same level reinforcing steel bars in both transverse and longitudinal beams are lumped and arranged in such a way that they can fit the FE mesh of the model at the particular level.

Analysis Assumptions

The following are the analysis assumptions made for the HCB models in this study to provide reasonably good simulations for the complex behavior:

- The bonds between each element/material type are assumed perfect. Unless the failure mode of a structure involves a bond failure, the perfect bond assumption used in the structural modeling will not cause a significant error in the predicted load-deflection response [13].
- Poisson's ratio is assumed to be constant throughout the loading history.
- The shear transfer coefficients in ANSYS for closed and open cracks in the SOLID65 element are assumed to be 1.0 and 0.2, respectively.
- Cracking controls the failure of the structures.
- The concrete material is assumed to be isotropic prior to cracking and orthotropic after cracking ([4], [13], [14]). The steel is assumed to be isotropic. The FRP material is assumed to be especially orthotropic-transversely isotropic. That is, the material properties in the two directions that are both perpendicular to the fiber direction are identical [15].
- Time-dependent nonlinearities such as creep, shrinkage, and temperature change are not included in this study.

Nonlinear Analysis in ANSYS

The status transition of concrete from an uncracked to cracked state and the nonlinear material properties of concrete in compression and steel as it yields cause the nonlinear behavior of the structures under loading. Newton-Raphson equilibrium iteration is used to solve nonlinear problems in ANSYS.

In a linear analysis the size of the load increment does not affect the results at all. However, for a nonlinear analysis, in which FE structures start cracking and behave nonlinearly under a sufficiently large load, the load applied to the structures must be increased gradually to avoid non-convergence. Tolerances in both force and displacement criteria may have to be gradually increased along the loading history to avoid a diverged solution.

Bridge Experiment and FE Modeling

Bridge Description

The Horsetail Creek Bridge was built in Oregon in 1914. The bridge with spread footing foundations is 18280 mm (60 ft.) long and 7315 mm (24 ft.) wide. It has three 6096-mm (20-foot) spans built across the Horsetail Creek. Due to structural deficiencies, strengthening of the structure was mandated [16]. The FRP strengthening was completed on the bridge in 1998 using both unidirectional CFRP and GFRP laminates, as earlier explained.

Loading Conditions and Field Data

Two different truck-loading levels are applied along the centerline of the bridge deck; i.e., empty and full truckloads. Strain data are collected for seven locations of the truck for both load levels. The positions of the truck depending on the distance of the front axle of the truck from the right end of the bridge, including the axle weights, are shown in Fig. 2. Note that the truck is shown only at positions 1 and 7 in Fig. 2.

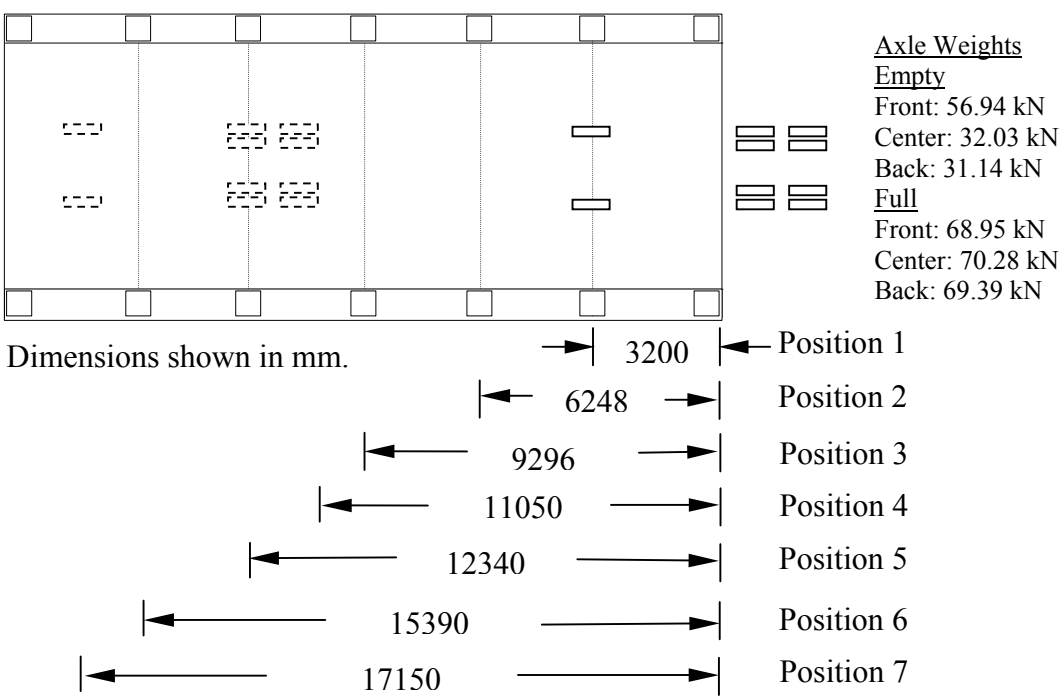

Fig. 2: Locations of loading trucks

Corrected field test data for the bridge was provided by the bridge owner (ODOT) [17]. However, only field test data collected after FRP strengthening are available. There is no control set of data available to represent the bridge's response prior to the retrofit. Fiber optic sensors have been attached on both the concrete and FRP laminates on the bottom and on the sides of the beams to measure strains occurring from the truck-loading tests. They are located on one transverse beam and one longitudinal beam of the HCB. In this paper, only the strain at the center bottom fiber of the concrete for the transverse beam at midspan (T0FC). The comparison between ANSYS predictions and the strain field data is made on the basis of an empty truckload applied on the HCB after retrofitting. The location of the transverse beam, on which the fiber optic sensor is attached, is shown in Fig. 3 (shaded areas).

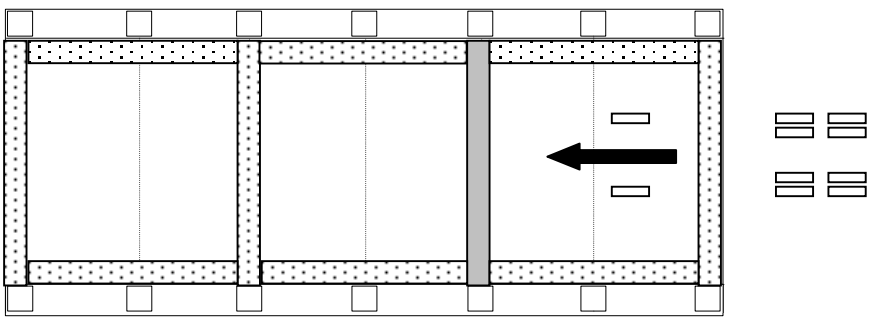

Fig. 3: Locations of the monitored beams

FE Bridge Modeling

The constitutive models, ANSYS elements, material properties, and assumptions previously discussed are used in the bridge analysis. Taking advantage of symmetry, only a longitudinal half of the bridge is modeled. The columns of the bridge are not modeled, and all degrees of freedom (DOF) at the locations of the columns are restrained instead. However, only vertical translation is restrained where the continuous walls are located (at both ends of the bridge). The numbers of elements used in the model are 9520 elements for concrete (SOLID65), 4354 element for steel bar (LINK8), and 1168 elements for FRP (SOLID46). The FE bridge model with steel reinforcement and FRP laminate details are shown in Fig. 4. and Fig. 5, respectively.

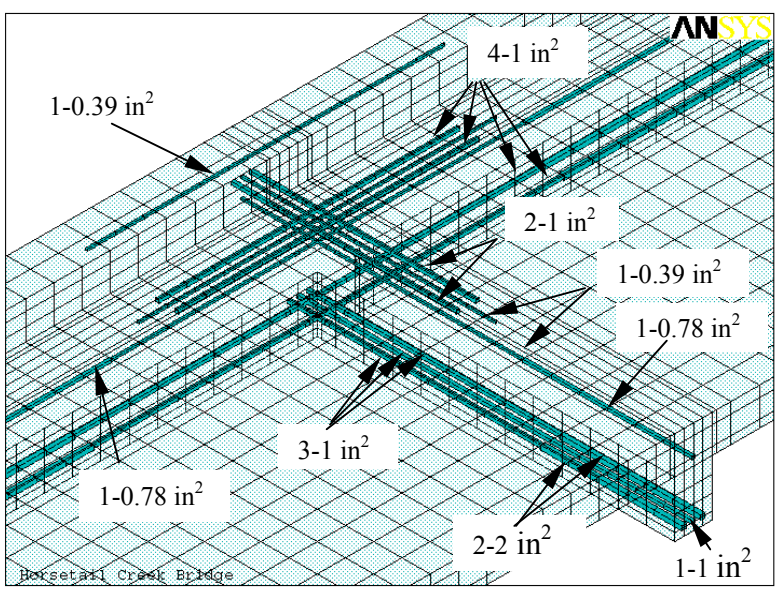

(a)

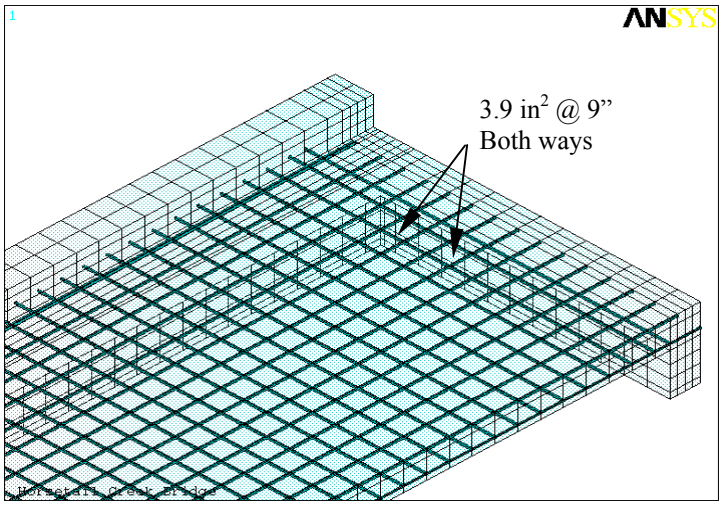

Fig. 4: Steel reinforcement details: (a) and (b) Typical reinforcement in the transverse and longitudinal beams and typical reinforcement in the bridge deck, respectively (1 in^2 = 645.2 mm^2).

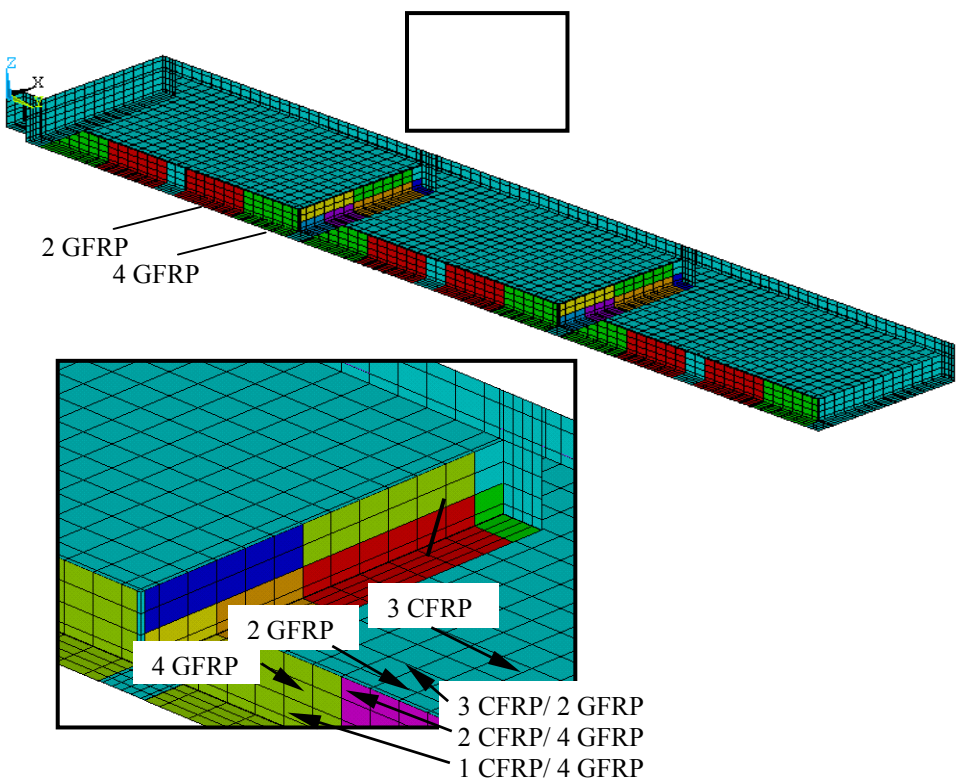

Fig. 5: FE Bridge Model Strengthening with FRP Laminates

Note that, for Fig. 4 (a), 1-0.78 in^2 represents one steel bar with an area of 0.78 in^2, while 2-2 in^2 represents two steel bars with an area of 2 in^2 for each bar, and so on. A standard size bar cannot be used because undeformed square bars were used in the actual bridge. For Fig. 5, 4 GFRP represents four layers of GFRP laminates, while 1 CFRP/4 GFRP represents a combination of one layer of CFRP laminate and four layers of GFRP laminates, and so on.

Results

Comparison of ANSYS Predictions with Field Data

On examining the ANSYS results for all of the truck positions, it was found that the bridge does not crack for the empty truckload. Therefore, the study is a linear analysis. It is, thus, possible to include the linear analysis results obtained from SAP2000 in these comparisons [18]. SAP2000 is another general-purpose finite element analysis program used to verify the ANSYS results in the linear analysis study [19]. A difference between the ANSYS and SAP2000 bridge FE models is that the 4420 mm long columns are included in SAP2000. This difference between these two models will affect comparison of the structural predictions between ANSYS and SAP2000. It is expected that the ANSYS bridge model will be stiffer than the SAP2000 model, as in SAP2000 model the columns are included which lowers the overall structural stiffness. The relatively large strains from the SAP2000 model are expected due to the lower structural stiffness. Also, in the SAP2000 analysis truss elements with isotropic material properties are used to represent the FRP laminates [18], which is not realistic and may reduce the overall structural stiffness compared to the SOLID46 elements with orthotropic material properties that are used to model the FRP laminates in ANSYS. The difference in the number of elements used in the ANSYS and SAP2000 models will also affect the solutions. After the symmetry condition is taken into account, the ANSYS model has about twice as many elements as the SAP2000 model.

Figs. 6 (a) shows comparisons of strains between the field data, ANSYS, and SAP2000 results [18] for various locations of the truck (Fig. 2). To better represent the effects of the moving truck on the structural behavior of the bridge, the strains are also plotted versus the distances of the single front axle of the truck from the end of the bridge (Fig. 2) and are shown in Fig. 6 (b). Basically, these plots are similar to "influence lines," but for a truck instead of a unit load. The field test data are based on average values between two test runs.

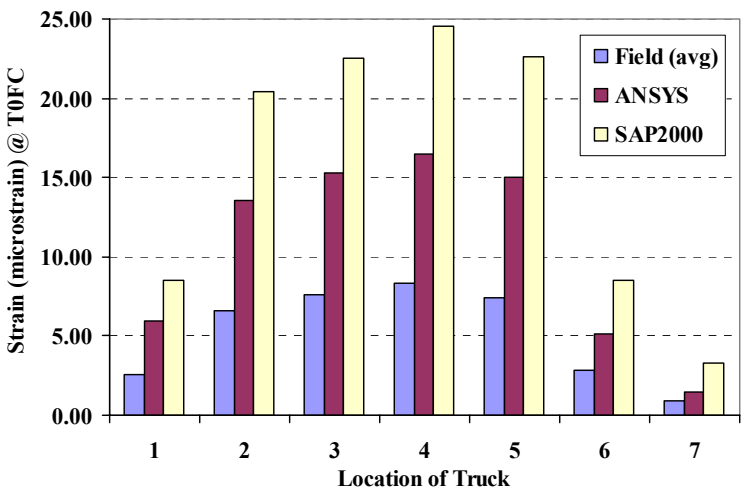

(a)

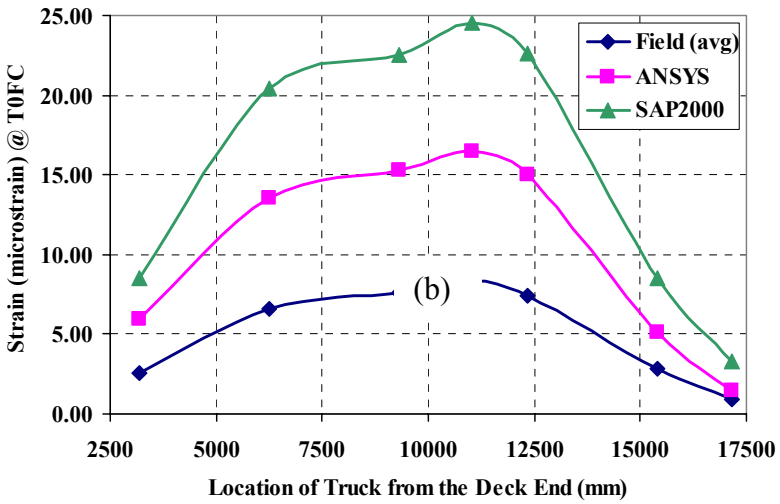

Fig. 6: Comparisons of strains (T0FC) between field data, ANSYS, and SAP2000 results: (a) At various truck locations (b) As function of the distance of the single axle from the end of the bridge deck.

As shown in Figs. 6 (a) and (b), both ANSYS and SAP2000 show similar trends to the field data. However, based on these field data, ANSYS predicts the behavior more accurately, as evident by the deviations. In additional, the ANSYS bridge model is stiffer than the SAP2000 model, as previously expected. From Fig. 6 (b), the maximum strain is obtained if the single axle of the truck is at 11050 mm (11.05 m) from the end of the bridge deck (Position 4 from Fig. 2) because at this location the loads from the middle tandem axles are right above the transverse beam, to which the fiber optic sensor is attached.

As seen in Figs. 6 (a) and (b), ANSYS very well predicts the trend in the strains versus the various truckload locations. Although the predicted trends are similar to those from the field test data, the differences between the ANSYS results and field test data are quite high, approximately from 60% up to 130%. Moreover, based on Figs. 6 (a) and (b), it is shown that the actual bridge is stiffer than the ANSYS bridge FE model, which is unexpected. Generally, an FE R/C model is stiffer than the actual R/C structure. One reason for this is because materials used to model the FE model are perfectly homogenous, unlike those in the actual structure. Moreover, the boundary conditions are strictly defined in the FE model, and the discretization itself imposes additional constraints on the displacements. These also tend to make the FE model stiffer. Additionally, in the actual R/C structure micro-cracks in the concrete and bond slip between the concrete and reinforcing steel bars, as well as other imperfections in construction, may lessen the stiffness of the actual structure. Furthermore, in this study the columns of the HCB were not modeled, which should also make the FE model considerably stiffer than the actual bridge.

However, the comparison seems to show that the actual bridge is stiffer than the model. One possible explanation is that the material properties of the concrete may be inaccurate. The 17.24 MPa (2500 psi) compressive strength of concrete used in the model complies with AASHTO bridge rating recommendations for all bridges built prior to 1959 [3]. The actual compressive strength of the concrete and modulus of elasticity are most likely substantially higher than the values used in the FE model. The concrete material properties are unknown unless the strength of the on-site concrete is tested using core samples, which the owner of the bridge has not been able to perform these tests on the historic structure.

This research provides estimates of the material properties of the in-situ concrete have recently conducted pulse-velocity tests. Analysis of these measurements is underway, but preliminary findings indicate that the concrete is not stiff enough to account for the differences between the test data and model predictions. The most reasonable explanation at this point seems to be that the currently available field test data may be inaccurate for some reason or not be correctly calibrated. Improvement in the comparisons may be obtained when a follow-on bridge test is conducted.

Analysis of the Unstrengthened HCB

Although field data representing behaviors of the HCB before the FRP strengthening are not available, it is interesting to examine the responses of the bridge before the retrofit using FE analysis. An unstrengthened bridge model is developed using the same methodology as for the strengthened bridge. The FE bridge model with steel reinforcement details prior to the retrofit is shown in Fig. 4. The empty truck loading is applied on the model for each location of the truck as in Fig. 2. Comparison of the strains for the FE bridge models with and without the FRP strengthening is made for the strains at the center bottom fiber of the concrete for the transverse beam at midspan (T0FC).

Differences in structural performance before and after retrofitting are not dramatic since the bridge does not crack under the applied truckload. Similar findings were shown in ([8], [9]) for the individual beams. However, after cracking, the beams strengthened with the FRP laminates showed noticeable improvements in structural performances by delaying the propagation of cracks and reducing the deflection of the beams. Thus, more significant improvements in overall bridge performance from the FRP are expected when the non-linear, cracking behavior is examined in a planned future study. The result of the comparison is shown in Table 2.

Table 2: Comparison of strains between FE bridge models with and without FRP strengthening

Locations (Distances from the end)	Strain (microstain)		
	T0FC		
	W/ FRP	W/O FRP	Diff. (%)
1 (3200)	5.979	6.280	-5.032
2 (6248)	13.57	14.20	-4.643
3 (9296)	15.27	16.04	-5.065
4 (11050)	16.51	17.32	-4.924
5 (12340)	15.03	15.77	-4.927
6 (13590)	5.105	5.375	-5.301
7 (17150)	1.467	1.556	-6.042

The unstrengthened bridge model does not crack under the empty truckload, and the analysis is thus linear. As expected, the differences in structural responses before and after the retrofit are not significant in the linear elastic behavior range.

Conclusions and Recommendations

Conclusions

The comparisons between ANSYS predictions and the experimental data show that the proposed FE models are good representations for both the HCB in terms of the number of elements, structural details, and, especially, reasonably accurate results in general. The HCB does not crack under the service applied truckload. Consequently, the uncracked bridge structure still behaves linearly. The trends in the strain results for the various locations of the truck obtained from both ANSYS and

SAP2000 models are similar to those from the field test data. However, the ANSYS strain results differ from the field strain data by approximately 60% up to 130%. This may be because of inaccurate material properties for the concrete or an incorrect strain calibration in the field. The FEM analysis shows that when the single axle of the empty truck is positioned at about 11.05 m from the end of the bridge deck, a maximum strain values is developed in the transverse beam. This is because the loads from the tandem axles strongly influence the beams when positioned at this location. For the influence of FRP strengthening, the differences in structural responses before and after the retrofit are not significant in the linear behavior range.

Recommendations

Recommendations from current research:

Generally, modeling a reinforced concrete structure in a nonlinear analysis (after cracking) in ANSYS is difficult. Reinforced concrete FE models either with or without FRP strengthening are very susceptible to numerical instability. Loads must be gradually applied to the structures. Tolerances for both force and displacement criteria must be closely monitored. Mesh size and shear transfer coefficient also affect solution convergence. The analysis of the HCB, however, is still linear due to the fact that the bridge does not crack under the applied truckload. Consequently, load increment size and shear transfer coefficient do not affect convergence difficulties except for mesh size that should be kept small enough to achieve accurate solutions.

Recommendations for further research:

To understand better how the FRP strengthening affects structural behaviors and improve structural performance of the HCB, a set of loads or distributed loads should be applied on the bridge model until its failure. The study of the HCB in the nonlinear range, including corrections of the field test data and actual concrete strength for the linear analysis of the HCB, is under investigation.

References

1. High Value State ODOT Research. (1999). "Keeping Oregon's Bridges Strong and Handsome." http://www4.nationalacademies.org/trb/scor/states.nsf/all/oregon.
2. Kachlakev, D.I. (1998). "Finite Element Method (FEM) Modeling for Composite Strengthening/Retrofit of Bridges." *Research Project Work Plan*, Corvallis, OR.
3. Consulting Engineers in conjunction with TAMS Consultants. (1997). "Evaluation and Resolution of Under Capacity State Bridges: Bridge #04543, Horsetail Creek Bridge." CH2M HILL, Inc., Corvallis, OR.
4. ANSYS User's Manual, Vol. I-IV; Revision 5.5. (1998). Swanson Analysis System, Inc., Houston, PA.
5. Bangash, M.Y.H. (1989). Concrete and Concrete Structures: Numerical Modeling and Applications. Elsevier Science Publishers, LTD., Essex, England.
6. William, K. J., and Warnke, E. P. (1975) "Constitutive Model for the Triaxial Behavior of Concrete," *Proceedings, International Association for Bridge and Structural Engineering*, Vol. 19, ISMES, Bergamo, Italy, 174.
7. ACI Committee 318. (1995). *Building Code Requirements for Standard Concrete (ACI 318-95) and Commentary (ACI 318R-95)*. ACI, Farmington Hills, MI.
8. Chansawat, K. (2000). "Nonlinear Finite Element Analysis of Reinforced Concrete Structures Strengthened with FRP Laminates." personal communications, Oregon State University Corvallis, OR.

9. Potisuk, T. (2000). "Finite Element Modeling of Reinforced Concrete Beams Externally Strengthened by FRP Composites." *MS Thesis*, Oregon State University, Corvallis, OR.
10. Kachlakev, D.I., and McCurry, D.Jr. (2000). "Testing of Full-Size Reinforced Concrete Beams Strengthened with FRP Composites: Experimental Results and Design Methods Verification." *SPR387*, *United States Department of Transportation Federal Highway Administration and the Oregon Department of Transportation*, Corvallis, OR.
11. Material Data Properties. (1998) *Tyfo Systems for Beams and Slabs*, Fyle Corporation LLC, San Diego, CA.
12. Kachlakev, D.I. (1998). "Strengthening Bridges Using Composite Materials." *SHWA-OR-RD-98-08*, *United States Department of Transportation Federal Highway Administration and the Oregon Department of Transportation*, Corvallis, OR.
13. Isenberg, J. (1993). *Finite Element Analysis of Reinforced Concrete Structures II*. ASCE, New York, NY.
14. Kant, T. (1985). *Finite Elements in Computational Mechanics*. 1, Pergamon Press, Inc., Elmsford, NY.
15. Hyer, M.W. (1998). Stress Analysis of Fiber-Reinforced Composite Materials. International ed. McGraw-Hill, Inc., Jurong, Singapore.
16. Kachlakev, D.I. (1999). "Retrofit of Historic Structures Using FRP Composites." *ICCE/6 Sixth Annual International Conference on Composites Engineering*, Orlando, FL, 387-388.
17. ODOT Field Test Data. (2000). *Private Correspondence*.
18. Kim, T.W. (2000). "3D Finite Element Analysis of Fiber-Reinforced Polymer Strengthened Reinforced Concrete Bridge." *MS Thesis*, Oregon State University, Corvallis, OR.